State-to-state measurements of the vibrational predissociation dynamics of $HeCl_2$

Joseph I. Cline, N. Sivakumar, Dwight D. Evard, and Kenneth C. Janda
Department of Chemistry, University of Pittsburgh, Pittsburgh, Pennsylvania 15260
(Received 16 March 1987)

Well-resolved state-to-state data are reported for the vibrational predissociation of specific rotational levels of $HeCl_2(B)$ with eight vibrational quanta in the Cl-Cl stretching mode. The state resolution is sufficient to clearly reveal the symmetry constraints on the dynamics as well as a node in the product-rotational-state distribution. "Parity-selected" excitation spectra are obtained which reduce spectral congestion and aid in the assignment of individual rovibronic transitions.

In the study of a chemical event, quantum state-to-state information is indispensable in order to clearly understand the mechanics of the time evolution of the system. Although true state-to-state data is very difficult to obtain, laser pump-probe techniques make it nearly possible to realize this goal. In this report we describe pump-probe studies of the vibrational predissociation of the $HeCl_2$ van der Waals molecule. The experiment is analogous to those previously reported for He- and NeICl,[1] and $NeCl_2$.[2] Because of more favorable rotational constants for $HeCl_2$ and better laser resolution it is possible to obtain truly state-to-state data for the first time. A "pump" laser pulse prepares a well-defined initial metastable rovibronic state of $HeCl_2$. Following dissociation, the population of individual rovibronic levels of the Cl_2 fragment is measured by a "probe" laser pulse. These data show that the parity of the initial state is conserved during the dissociation so that the relationship between the intramolecular potential and the dynamics is immediately apparent from the data. The conservation of parity can be used to clarify the excitation spectra by detecting either even- or odd-parity states. This parity-selected excitation spectroscopy not only reduces spectral congestion, but also greatly aids the assignment of individual transitions. Two distinct maxima are observed in the product-rotational-state distributions indicating the presence of a "half-collision" rotational rainbow or quantum interference among the product-state channels. The data can be directly compared to studies[2] of the vibrational predissociation of $NeCl_2$ in order to test how the dynamics depend upon the mass of the rare-gas atom and the intramolecular potential-energy surface.

$HeCl_2$ was prepared in a pulsed free jet expansion (150-μm-diameter nozzle) of a mixture of 0.6% Cl_2 in He at a total pressure of 350 psi. The mixture was obtained by passing He over a vessel containing liquid Cl_2 at $-77\,^{\circ}C$. The rotational temperature of van der Waals molecules formed in the jet was approximately 0.6 K. Two dye lasers, pumped by an excimer laser (XeCl), provided tunable pump (ω_1) and probe (ω_2) laser pulses which were propagated colinearly through the vacuum apparatus and perpendicular to the free jet expansion. The dye laser providing the ω_1 pulse was operated with an intracavity etalon to produce $\sim$20-ns pulses at 0.05 cm^{-1} band width. The output of the probe dye laser was frequency doubled in KPB (potassium pentaborate) to produce $\sim$20-ns pulses at $\sim$0.2 cm^{-1} bandwidth. A Schott UG-5 filter attenuated the fundamental of the second laser. The ω_2 pulse was delayed $\sim$10 ns from the ω_1 pulse. uv fluorescence was imaged onto a photomultiplier, while a Corning 7-54 filter rejected visible laser scatter. The ω_2 pulse energy was monitored by reflecting a portion of the uv beam through a dye cell viewed by a photodiode. Gated integrators averaged the photodiode and photomultiplier signals. A microcomputer controlled the synchronization of the pulsed valve, laser trigger, and detection electronics, scanned the dye-laser gratings, etalon, and doubling crystal, and recorded the data.

The pump-laser frequency, ω_1, was tuned to prepare a vibronically excited, metastable state of $HeCl_2$ with eight quanta of vibration in the Cl-Cl stretching mode. This vibronic state of $HeCl_2$ is associated with the long-lived Cl_2 (B, $v=8$) state. $HeCl_2$ has been observed in laser-excited fluorescence studies[3] approximately 3 cm^{-1} to the blue of the Cl_2 $B\,^3\Pi(0_u^+)\leftarrow X\,^1\Sigma_g^+$ ($8\leftarrow 0$) transition.[4] By scanning the laser through the rotational structure of the band, specific rotational levels of $HeCl_2(B,\ v=8)$ were prepared. The He atom is so weakly bonded to the Cl_2 molecule that even one quantum of the Cl-Cl vibrational stretch has sufficient energy to cause decomposition. Intramolecular vibrational energy redistribution results in decay of the prepared state with a lifetime of 506 ± 77 ps as estimated by homogeneous linewidth studies.[3] The quantum state of the $Cl_2(B)$ fragment was determined by tuning ω_2 through the Cl_2 $E(0_g^+)\leftarrow B\,^3\Pi(0_u^+)$ transition.[5] For both excitation spectra and product-distribution measurements, fluorescence from the Cl_2 E state is detected as a function of ω_1 and ω_2.

The $Cl_2(B)$ fragments from decomposition of $HeCl_2(B,v=8)$ were observed to be in the $v=7$ vibrational quantum state with negligible signal observed for $v\leq 6$. Figure 1(a) shows a spectrum recorded by setting ω_2 on the bandhead of the $^{35}Cl_2$ $E\leftarrow B$ ($0\leftarrow 7$) transition and tuning the pump laser, ω_1, through the He $^{35}Cl_2$ $B\leftarrow X$ ($8\leftarrow 0$) band. This spectrum is similar to the visible fluorescence excitation spectrum previously reported.[3] The rotational structure in the band contour can be simulated by a T-shaped, rigid-top Hamiltonian for $HeCl_2$ in which the He atom lies along the perpendicular bisector of

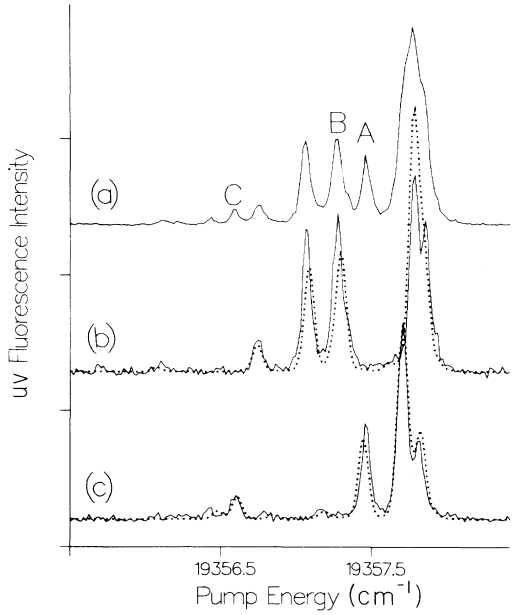

FIG. 1. Solid curves are spectra of He $^{35}Cl_2$ obtained by scanning ω_1 through the $HeCl_2$ $B \leftarrow X$ (8←0) band and (a) positioning ω_2 on the bandhead of the $^{35}Cl_2$ $E \leftarrow B$ (0←7) transition, (b) positioning ω_2 on the $P(10)$ line of the $^{35}Cl_2$ $E \leftarrow B$ (0←7) band, and (c) positioning ω_2 on the $P(9)$ line. Dotted curves are calculated asymmetric-top spectra for transitions to only (b) even- or (c) odd-parity rotational states of He $^{35}Cl_2(B,v=8)$ The rigid, T-shaped model has He to Cl_2 center-of-mass distances of 3.67 and 3.79 Å and Cl-Cl distances of 1.99 and 2.64 Å in the X and B electronic states, respectively. The linewidth is set to that of Ref. 2 and the Boltzman rotational temperature is 0.6 K.

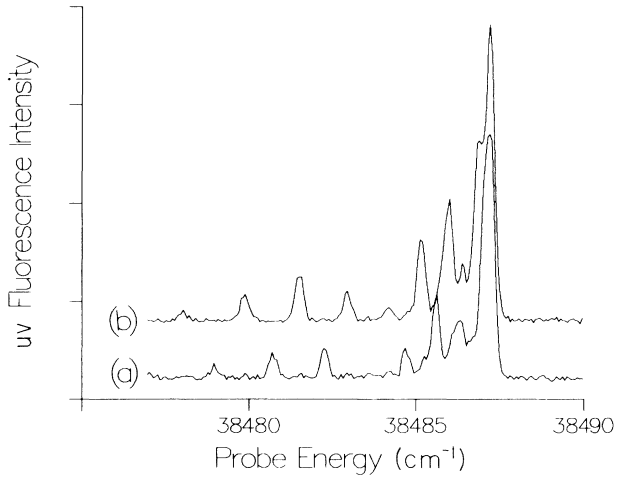

FIG. 2. Pump-probe spectra obtained by scanning ω_2 through the fragment $^{35}Cl_2$ $E \leftarrow B$ (0←7) band and (a) positioning ω_1 on feature A of Fig. 1(a) [the He $^{35}Cl_2$ $B \leftarrow X$ ($8 \leftarrow 0$, $1_{10} \leftarrow 1_{11}$) transition] and (b) positioning ω_1 on feature B of Fig. 1(a) [the $B \leftarrow X$ ($8 \leftarrow 0$, $1_{11} \leftarrow 1_{10}$) transition]. These spectra reveal the quantum state of the fragment $^{35}Cl_2$ following decomposition of (a) the $J_{k_p k_0} = 1_{10}$ and (b) 1_{11} rotational levels of He $^{35}Cl_2(B,v=8)$.

the Cl-Cl bond axis. In this model the He to Cl_2 center-of-mass distance, R, in the B electronic state is $R_B = 3.9 \pm 0.4$ Å and the difference in R for the X and B electronic states is $R_B - R_X = 0.127 \pm 0.024$ Å. The Cl-Cl bond length in both electronic states is fixed to values obtained from the rotational constants, B_v, of free Cl_2.[4] The a inertial axis of the asymmetric top model is parallel to the Cl-Cl bond axis and the b inertial axis lies in the molecular plane and passes through the He atom. A simulated $HeCl_2$ $B \leftarrow X$ (8←0) spectrum calculated using this asymmetric top analysis assigns the intense feature on the blue side of the band to several overlapping rovibronic transitions (the "bandhead"), whereas the weaker features to the red result from nearly unblended transitions.

Figure 2 shows spectra obtained by setting ω_1 on the features labeled A and B in Fig. 1(a) and tuning the probe laser, ω_2, through the $^{35}Cl_2$ $E \leftarrow B$ (0←7) band (the assignment of the A and B features will be discussed below). Both of the $^{35}Cl_2$ fragment spectra consist of an R branch head and a well-resolved P branch which extends to the red of the bandhead. When the pump laser is positioned on feature A, probe-laser transitions are observed originating from $j = 1$, 3, 5, 9, 11, and 13 of the $^{35}Cl_2(B,v=7)$ fragment. Similarly, upon excitation of B, transitions are observed originating from $j = 0$, 2, 4, 6, 8, 10, 12, and 14 of the $^{35}Cl_2(B,v=7)$ fragment.

Two features of Fig. 2 are particularly interesting. First, it is apparent that specific metastable rotational states of $He^{35}Cl_2$ decay into fragment states of either even or odd j, i.e., of either even or odd parity with respect to exchange of the two ^{35}Cl atoms. However, when the ω_1 frequency is set to the bandhead of the $He^{35}Cl_2$ spectrum (so that several rotational levels are excited) both even- and odd-parity product states are observed. Second, the intensity of transitions in the fragment $^{35}Cl_2$ rotational branches peaks at $j = 3$ with a second maximum between $j = 9$ and 10. Between the two maxima, the intensity becomes negligible at $j = 7$. Rotational-state population distributions obtained from the data of Fig. 2 are presented in Fig. 3.

It is clear that only fragment rotational quantum states of definite parity are produced in the vibrational predissociation from a given initial rotational quantum state of the metastable molecule. These results indicate that the quantum state prepared by the ω_1 pulse has definite parity and that the parity is conserved in the dissociation reaction. The vibrational predissociation is analogous to a rotationally and vibrationally inelastic scattering event for which the nuclear spin state, and hence the parity, of $^{35}Cl_2$ would be expected to be conserved. As shown in Fig. 4, the vibrational predissociation of $He^{35}Cl^{37}Cl(B,\ v=8)$ also gives rise to only even or odd j $^{35}Cl^{37}Cl(B,\ v=7)$ fragment rotational states when a specific initial rotational state is prepared by the ω_1 pulse. The heteronuclear diatomic need not have definite parity, but the intramolecular van der Waals potential should remain nearly symmetric with respect to the parity operation. This demonstrates that the symmetry of the $HeCl_2$ intramolecular potential is responsible for selection rules in the decomposition dynamics which couple specific ini-

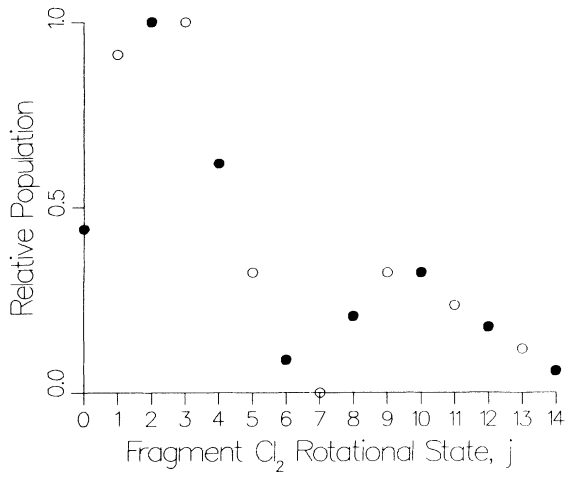

FIG. 3. $^{35}Cl_2$ fragment rotational quantum-state population distributions obtained from the spectra of Fig. 2. Populations were extracted by simulation of the 0←7 vibrational band using the spectroscopic constants of Ref. 4. Filled circles are for decomposition of the 1_{11} rotational level of $He^{35}Cl_2(B, v=8)$ [Fig. 2(a)]. Open circles are for decomposition of the 1_{10} rotational level [Fig. 2(b)].

tial metastable states of $HeCl_2$ to continuum product rotational states of a specific symmetry.

The unusual product rotational-state population distributions of Figs. 2 and 3 show features which undoubtedly reflect details of the potential energy surface of the molecule. Both the even- and odd-parity rotational-state population distributions are peaked at low j, with a second maximum in the distribution at $j=9$ and 10. These features are similar to rotational rainbows observed in the direct dissociation of molecules on repulsive potential energy surfaces.[6,7] Alternatively, they may indicate a quantum-interference effect. The population distribution depends slightly upon the rotational state prepared by the ω_1 pulse. In particular, excitation of feature A of Fig. 1(a) gives rise to odd j states with no measurable population of the $j=7$ level, whereas excitation of feature C gives rise to odd j products with the population of the $j=7$ level comparable to that of $j=13$. Combining these product-state distributions with close-coupling calculations, constrained by the structural information obtained from the rotational assignments of the excitation spectra, should lead to a detailed potential energy surface. This work is in progress.

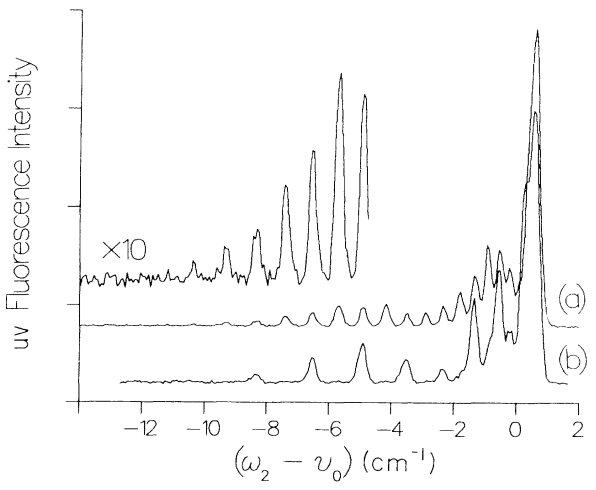

FIG. 4. Spectra of $He^{35}Cl^{37}Cl$ obtained by scanning ω_2 through the fragment $^{35}Cl^{37}Cl$ E←B (0←7) band and (a) positioning ω_1 on the bandhead of the $He^{35}Cl^{37}Cl$ B←X (8←0) transition and (b) positioning ω_1 to prepare the 1_{11} rotational level of $He^{35}Cl^{37}Cl(B, v=8)$.

By positioning the probe frequency to detect a single even or odd j $Cl_2(B, v=7)$ fragment rotational state and then tuning the pump laser, only transitions to either even- or odd-parity rotational states of $HeCl_2$ are observed in the excitation spectra. Such spectra are presented for $He^{35}Cl_2$ in Figs. 1(b) and 1(c). Similar spectra are observed for the $He^{35}Cl^{37}Cl$ species. These symmetry-resolved spectra permit unambiguous assignment of individual transitions not only as a result of the reduced spectral congestion but also by providing an additional constraint upon the identity of the states: their parity. The parity of the $HeCl_2$ asymmetric-top rotational wave functions is given by their behavior upon operation of the C_2 symmetry rotation about the b axis of the inertia ellipsoid. All of the features in Figs. 1(b) and 1(c) can be labeled as a-type asymmetric-top rotational transitions[8] and are consistent with the previous asymmetric-top analysis of the $He^{35}Cl_2$ B←X (8←0) band contour. In particular, features A, B, and C of Fig. 1(a) are assigned to the 1_{10}←1_{11}, 1_{11}←1_{10}, and 1_{01}←2_{02} rotational transitions, respectively (where $J_{k_p k_0}$ labels the asymmetric-top rotational levels involved in the vibronic transition). The reduced congestion in the symmetry-resolved excitation spectra permits the measurement of small, but significant, deviations from calculated spectra based on the rigid, T-shaped model (see Fig. 1). However, it remains surprising that a rigid model should work so well for what must certainly be a very floppy molecule. These results imply that the rotational spectroscopy of $HeCl_2$ can be described in terms of some effective average rigid structure. More refined models for the $HeCl_2$ vibrational-rotational energy levels will be critically tested by these data.

Comparison of these results to those recently reported[2] for the vibrational predissociation of $NeCl_2$ shows that the decomposition dynamics for the two molecules is quite different. Fragment quantum-state distributions for the vibrational predissociation of $NeCl_2(B, v=11)$ show that, as in $HeCl_2$, the loss of one Cl_2 vibrational quantum is by far the most favorable relaxation channel. However, the vibrational predissociation of $NeCl_2$ yields all fragment rotational states consistent with conservation of energy, parity, and angular momentum. The energy of the highest observed rotational state ($j_{max}=24$) is roughly 85% of the total available energy and corresponds to a classical half-collision impact parameter of ~ 7.2 Å.[2] In contrast to $NeCl_2$, where the rotational distribution terminates abruptly at $j=24$, the Cl_2 product rotational population distribution for $HeCl_2$ decays gradually to unobservable

levels for $j > 16$. This is much lower than dictated by the constraints of conservation of energy and angular momentum. Using a potential energy surface determined by crossed-beams scattering data,[9] the dissociation energy, D_0, of $HeCl_2$ is estimated[10] to be $\sim 12 \pm 4$ cm^{-1}. The amount of energy available to go into Cl_2 rotational energy and relative translational kinetic energy is the energy of the eighth vibrational quantum (175 cm^{-1}) minus D_0. Using this estimate, $j_{max} = 16$ accounts for roughly 24% of the available energy and corresponds to an impact parameter of 3 Å.

In conclusion, we have reported state-to-state data for the vibrational predissociation of $HeCl_2$. The results clearly show parity conservation during evolution of the wave function in the decomposition process. Two maxima and an intervening node are observed in the Cl_2 fragment rotational distribution indicating the possibility of a rotational rainbow or quantum interference in the dynamics. By obtaining similar data for several Cl_2 vibrational levels we will be able to determine a detailed potential energy surface for this molecule.

This research was supported by the National Science Foundation, Grant No. CHE-8519057.

[1]J. M. Skene, J. C. Drobits, and M. I. Lester, J. Chem. Phys. **85**, 2329 (1986).
[2]J. I. Cline, N. Sivakumar, D. D. Evard, and K. C. Janda, J. Chem. Phys. **86**, 1636 (1987).
[3]J. I. Cline, D. D. Evard, F. Thommen, and K. C. Janda, J. Chem. Phys. **84**, 1165 (1986).
[4]J. A. Coxon, J. Mol. Spectrosc. **82**, 264 (1980).
[5]T. Ishiwata, T. Shinzawa, T. Kusayanagi, and I. Tanaka, J. Chem. Phys. **82**, 1788 (1985).
[6]K. Sato, Y. Achiba, H. Nakamura, and K. Kimura, J. Chem. Phys. **85**, 1418 (1986).
[7]R. Schinke, J. Chem. Phys. **85**, 5049 (1986).
[8]G. Herzberg, *Molecular Spectra and Molecular Structure* (van Nostrand Reinhold, New York, 1966), Vol. III, Chap. II3d.
[9]M. J. O'Loughlin, Ph.D. thesis, California Institute of Technology, 1986.
[10]B. P. Reid (private communication).